Crystal structure of citalopram hydrobromide, $C_{20}H_{22}FN_2OBr$

James A. Kaduk,[1,a] Kai Zhong,[2] Amy M. Gindhart,[2] and Thomas N. Blanton[2]
[1]*Illinois Institute of Technology, 3101 S. Dearborn St., Chicago, Illinois 60616*
[2]*ICDD, 12 Campus Blvd., Newtown Square, Pennsylvania 19073-3273*

(Received 24 October 2015; accepted 23 March 2016)

The crystal structure of citalopram hydrobromide has been solved and refined using synchrotron X-ray powder diffraction data, and optimized using density functional theory techniques. Citalopram hydrobromide crystallizes in space group $P2_1/c$ (#14) with $a = 10.766\,45(6)$, $b = 33.070\,86(16)$, $c = 10.892\,85(5)$ Å, $\beta = 90.8518(3)°$, $V = 3878.03(4)$ Å^3, and $Z = 8$. N–H···Br hydrogen bonds are important to the structure, but the crystal energy is dominated by van der Waals attraction. The powder pattern was submitted to International Centre for Diffraction Data for inclusion in the Powder Diffraction File™. © *2016 International Centre for Diffraction Data.* [doi:10.1017/S0885715616000178]

Key words: citalopram hydrobromide, Celexa, Cipramil, powder diffraction, Rietveld refinement, density functional theory

I. INTRODUCTION

Citalopram hydrobromide (tradenames include Celexa and Cipramil), is used in the treatment of depression. Citalopram hydrobromide is a selective serotonin reuptake inhibitor, and is administered in tablet form. The systematic name (CAS Registry number 59729-32-7) is (*RS*)-1-[3-dimethylamino)propyl]-1-(4-fluorophenyl)-1,3-dihydroisobenzofuran-5-carbonitrile hydrobromide. A two-dimensional (2D) molecular diagram is shown in Figure 1. Crystallization of citalopram salts, including the hydrobromide, is claimed in US Patent 4,650,884 (Bogeso and Lundbeck, 1987), but no powder diffraction patterns are provided. Crystals of citalopram hydrobromide and methods for preparing them are claimed in European Patent Application 1,152,000 (Ikemoto *et al.*, 2001), and powder diffraction patterns (but no crystal structures) are reported. The presence of high-quality reference powder patterns in the Powder Diffraction File (PDF;ICDD, 2015) is important for phase identification, particularly by pharmaceutical, forensic, and law enforcement scientists. The crystal structures of a significant fraction of the largest dollar volume pharmaceuticals have not been published, and thus calculated powder patterns are not present in the PDF-4 databases. Sometimes experimental patterns are reported, but they are generally of low quality. This structure is a result of a collaboration among ICDD, Illinois Institute of Technology (IIT), Poly Crystallography Inc., and Argonne National Laboratory to measure high-quality synchrotron powder patterns of commercial pharmaceutical ingredients, include these reference patterns in the PDF, and determine the crystal structures of these active pharmaceutical ingredients (APIs).

Even when the crystal structure of an API is reported, the single-crystal structure was often determined at low temperature. Most powder measurements are performed at ambient conditions. Thermal expansion (generally anisotropic) means that the peak positions calculated from a low-temperature single-crystal structure often differ significantly from those measured at ambient conditions, even if the structure remains the same. These peak shifts can result in failure of default search/match algorithms to identify a phase, even when it is present in the sample. High-quality reference patterns measured at ambient conditions are thus critical for easy identification of APIs using standard powder diffraction practices.

II. EXPERIMENTAL

Citalopram hydrobromide was commercial reagent, purchased from Sigma-Aldrich (Lot No. SLBG5276V), and was used as-received. The white powder was packed into a 1.5 mm diameter Kapton capillary, and rotated during the measurement at ~50 cycles s^{-1}. The powder pattern was measured at 295 K at beam line 11-BM (Lee *et al.*, 2008; Wang *et al.*, 2008) of the Advanced Photon Source at Argonne National Laboratory using a wavelength of 0.413 676 Å from 0.5 to 50° 2θ with a step size of 0.001° and a counting time of 0.1 s step^{-1}. The pattern was indexed on a primitive monoclinic unit cell having $a = 10.872$, $b = 33.274$, $c = 10.933$ Å, $\beta = 90.884°$, $V = 3955.0$ Å^3, and $Z = 8$ using

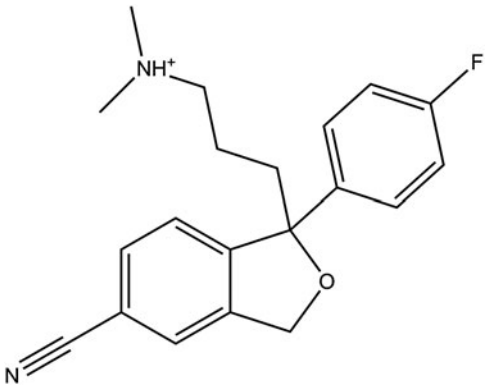

Figure 1. The molecular structure of the citalopram cation.

[a]Author to whom correspondence should be addressed. Electronic mail: kaduk@polycrystallography.com

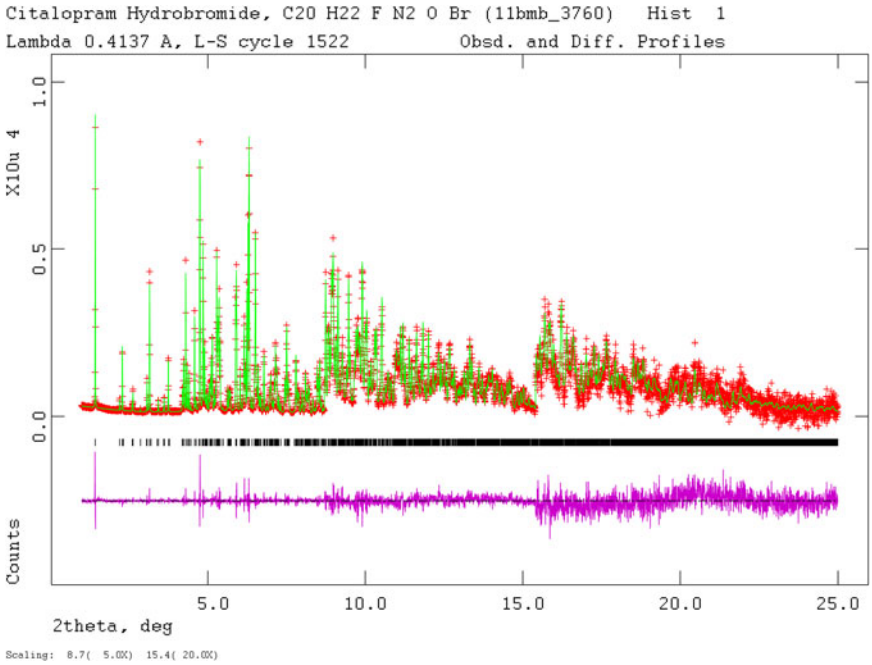

Figure 2. (Color online) The Rietveld plot for the refinement of citalopram hydrobromide. The red crosses represent the observed data points, and the green line is the calculated pattern. The magenta curve is the difference pattern, plotted at the same vertical scale as the other patterns. The vertical scale has been multiplied by a factor of 5 for $2\theta > 8.7°$, and by a factor of 20 for $2\theta > 15.4°$.

TABLE I. Rietveld refined crystal structure of citalopram hydrobromide.

Crystal data	
$C_{20}H_{22}BrFN_2O$	$\beta = 90.8518\ (3)°$
$M_r = 405.31$	$V = 3878.03\ (2)$ Å^3
Monoclinic, $P2_1/c$	$Z = 8$
$a = 10.766\ 45\ (6)$ Å	synchrotron radiation, $\lambda = 0.413\ 676$ Å
$b = 33.070\ 86\ (16)$ Å	$T = 293$ K
$c = 10.892\ 85\ (5)$ Å	
Data collection	
11-BM APS diffractometer	
Refinement	
Least-squares matrix: full	49 497 data points
$R_p = 0.052$	Profile function: CW Profile function number 4 with 21 terms Pseudovoigt profile coefficients as parameterized in Thompson *et al.* (1987). Asymmetry correction of Finger *et al.* (1994). Microstrain broadening by Stephens (1999). #1(GU) = 1.163 #2 (GV) = −0.126 #3(GW) = 0.063 #4(GP) = 0.000 #5(LX) = 0.323 #6(ptec) = 0.00 #7(trns) = 0.00 #8(shft) = 0.0000 #9(sfec) = 0.00 #10(S/L) = 0.0011 #11(H/L) = 0.0011 #12(eta) = 0.2951 #13 (S400) = 2.8×10^{-2} #14(S040) = 9.1×10^{-5} #15(S004) = 1.3×10^{-2} #16(S220) = 2.2×10^{-3} #17(S202) = 8.2×10^{-3} #18(S022) = 4.0×10^{-3} #19(S301) = -1.2×10^{-2} #20(S103) = -7.0×10^{-3} #21(S121) = 3.8×10^{-3} Peak tails are ignored where the intensity is below 0.0020 times the peak Aniso. broadening axis 0.0 0.0 1.0
$R_{wp} = 0.063$	184 parameters
$R_{exp} = 0.048$	138 restraints
$R(F^2) = 0.074\ 27$	$(\Delta/\sigma)_{max} = 0.03$
$\chi^2 = 1.850$	Background function: GSAS Background function number 1 with three terms. Shifted Chebyshev function of first kind 1: 124.973 2: 158.141 3: −71.0001

Fractional atomic coordinates and isotropic displacement parameters (Å^2)

	x	y	z	U_{iso}*/U_{eq}
C1	0.6384 (3)	0.907 93 (8)	0.6246 (3)	0.0577 (4)*
C2	0.4387 (3)	0.960 59 (9)	0.6099 (3)	0.0577 (4)*
C3	0.5711 (3)	0.911 51 (8)	0.5162 (3)	0.0577 (4)*
C4	0.6067 (3)	0.930 60 (10)	0.7268 (3)	0.0577 (4)*
C5	0.5070 (4)	0.956 93 (9)	0.7198 (3)	0.0577 (4)*

Continued

https://doi.org/10.1017/S0885715616000178 Published online by Cambridge University Press

TABLE I. Continued

	x	y	z	U_{iso}*/U_{eq}
C6	0.4716 (3)	0.937 69 (9)	0.5085 (3)	0.0577 (4)*
C7	0.3397 (8)	0.9898 (3)	0.5996 (4)	0.0584 (5)*
N8	0.2618 (7)	1.0132 (2)	0.5951 (5)	0.0584 (5)*
C9	0.6271 (6)	0.8846 (3)	0.4213 (4)	0.0584 (5)*
O10	0.7389 (4)	0.869 88 (16)	0.4777 (4)	0.0577 (4)*
C11	0.7335 (4)	0.874 47 (12)	0.6091 (4)	0.0577 (4)*
C12	0.8607 (3)	0.888 29 (9)	0.6558 (3)	0.0577 (4)*
C13	0.9144 (4)	0.872 41 (8)	0.7616 (3)	0.0584 (5)*
C14	0.9251 (4)	0.917 78 (9)	0.5926 (3)	0.0584 (5)*
C15	1.0396 (4)	0.931 21 (8)	0.6331 (3)	0.0577 (4)*
C16	1.0291 (4)	0.885 47 (9)	0.8037 (3)	0.0577 (4)*
C17	0.6889 (5)	0.834 88 (14)	0.6664 (6)	0.0577 (4)*
C18	0.7667 (7)	0.797 74 (18)	0.6396 (9)	0.0577 (4)*
C19	0.7122 (7)	0.7633 (2)	0.7087 (7)	0.0577 (4)*
N20	0.7665 (5)	0.723 61 (17)	0.6789 (6)	0.0577 (4)*
C21	0.6724 (8)	0.6966 (3)	0.6208 (8)	0.0577 (4)*
C22	0.8183 (8)	0.7038 (3)	0.7904 (8)	0.0577 (4)*
F23	1.2045 (4)	0.926 59 (17)	0.7752 (5)	0.0584 (5)*
C24	1.0887 (3)	0.914 63 (9)	0.7379 (3)	0.0584 (5)*
C25	0.0443 (3)	0.585 21 (10)	0.6975 (2)	0.0584 (5)*
C26	−0.1511 (3)	0.544 66 (12)	0.5855 (2)	0.0584 (5)*
C27	0.0283 (3)	0.544 49 (10)	0.7182 (2)	0.0577 (4)*
C28	−0.0373 (3)	0.606 08 (11)	0.6205 (2)	0.0584 (5)*
C29	−0.1348 (3)	0.585 98 (13)	0.5645 (2)	0.0584 (5)*
C30	−0.0691 (3)	0.524 10 (11)	0.6625 (3)	0.0577 (4)*
C31	−0.2531 (7)	0.523 80 (15)	0.5290 (10)	0.0584 (5)*
N32	0.3360 (5)	0.508 42 (18)	0.4833 (8)	0.0584 (5)*
C33	0.1315 (6)	0.529 56 (12)	0.7999 (7)	0.0577 (4)*
O34	0.1926 (4)	0.565 31 (15)	0.8430 (4)	0.0584 (5)*
C35	0.1566 (3)	0.599 87 (12)	0.7702 (4)	0.0584 (5)*
C36	0.2625 (3)	0.610 96 (12)	0.6848 (2)	0.0577 (4)*
C37	0.4426 (3)	0.629 06 (11)	0.5178 (2)	0.0584 (5)*
C38	0.3520 (4)	0.582 67 (11)	0.6542 (3)	0.0577 (4)*
C39	0.2664 (3)	0.648 70 (12)	0.6288 (3)	0.0584 (5)*
C40	0.3565 (4)	0.658 07 (10)	0.5447 (3)	0.0584 (5)*
C41	0.4428 (3)	0.591 46 (11)	0.5704 (3)	0.0584 (5)*
C42	0.1209 (5)	0.634 41 (17)	0.8560 (5)	0.0577 (4)*
C43	0.2174 (6)	0.6452 (3)	0.9537 (8)	0.0584 (5)*
C44	0.1660 (6)	0.6778 (3)	1.0361 (7)	0.0584 (5)*
N45	0.2635 (6)	0.697 69 (19)	1.1142 (5)	0.0584 (5)*
C46	0.2132 (8)	0.7312 (3)	1.1896 (8)	0.0577 (4)*
C47	0.3344 (8)	0.6686 (3)	1.1936 (8)	0.0577 (4)*
F48	0.5340 (4)	0.638 23 (15)	0.4356 (5)	0.0577 (4)*
Br49	0.984 83 (14)	0.714 38 (4)	0.480 47 (12)	0.0655 (4)*
Br50	0.4629 9 (14)	0.770 12 (4)	0.419 46 (12)	0.0655 (4)*
H51	0.649 99	0.926 86	0.810 31	0.0743 (4)*
H52	0.474 99	0.975 21	0.799 07	0.0743 (4)*
H53	0.416 39	0.940 55	0.418 83	0.0750 (5)*
H54	0.554 89	0.860 67	0.389 81	0.0750 (5)*
H55	0.867 44	0.846 45	0.804 75	0.0750 (5)*
H56	0.8834	0.931 43	0.505 18	0.0743 (4)*
H57	1.081 67	0.956 21	0.581 06	0.0743 (4)*
H58	1.071 26	0.870 02	0.875 47	0.0743 (4)*
H59	0.591 04	0.827 78	0.631 28	0.0750 (5)*
H60	0.674 56	0.839 27	0.761 93	0.0750 (5)*
H61	0.866 68	0.803	0.671 64	0.0743 (4)*
H62	0.764 04	0.791 34	0.536 76	0.0743 (4)*
H63	0.727 27	0.768 34	0.811 39	0.0743 (4)*
H64	0.608 08	0.762 22	0.6884	0.0743 (4)*
H65	0.720 78	0.673 88	0.559	0.0743 (4)*
H66	0.6199	0.679 76	0.695 17	0.0743 (4)*
H67	0.6043	0.715 43	0.563 64	0.0743 (4)*
H68	0.866 03	0.727 36	0.851 11	0.0743 (4)*
H69	0.888 71	0.679 84	0.762 61	0.0750 (5)*
H70	0.743 55	0.692 74	0.850 59	0.0750 (5)*
H71	0.848 78	0.726 07	0.622 57	0.0750 (5)*

Continued

https://doi.org/10.1017/S0885715616000178 Published online by Cambridge University Press

TABLE I. Continued

	x	y	z	U_{iso}*/U_{eq}
H72	−0.015 44	0.638 49	0.5921	0.0750 (5)*
H73	−0.194 18	0.602 54	0.496 85	0.0743 (4)*
H74	−0.084 58	0.491 48	0.674 85	0.0750 (5)*
H75	0.190 48	0.507 11	0.760 37	0.0750 (5)*
H76	0.088 79	0.515 44	0.884 17	0.0743 (4)*
H77	0.348 11	0.551 94	0.684 68	0.0750 (5)*
H78	0.208 65	0.673 52	0.647 98	0.0750 (5)*
H79	0.380 17	0.689 79	0.507 37	0.0743 (4)*
H80	0.515 12	0.567 67	0.539 45	0.0750 (5)*
H81	0.038 39	0.623 02	0.901 36	0.0750 (5)*
H82	0.091 04	0.660 13	0.799 24	0.0743 (4)*
H83	0.305 02	0.656 76	0.9078	0.0750 (5)*
H84	0.252 03	0.619 36	0.996 83	0.0743 (4)*
H85	0.098 55	0.6651	1.094 43	0.0750 (5)*
H86	0.127 96	0.703 28	0.984 56	0.0750 (5)*
H87	0.1481	0.718 12	1.257 56	0.0750 (5)*
H88	0.165 92	0.7513	1.129 51	0.0743 (4)*
H89	0.289 75	0.7455	1.241 96	0.0750 (5)*
H90	0.421 34	0.658 35	1.143 95	0.0750 (5)*
H91	0.362 29	0.684 12	1.283 36	0.0750 (5)*
H92	0.273 64	0.641 29	1.214 04	0.0743 (4)*
H93	0.333 82	0.709 02	1.059 43	0.15 (4)*
H94	0.641 83	0.902 42	0.332 31	0.15 (4)*

TABLE II. DFT-optimized (CRYSTAL14) crystal structure of citalopram hydrobromide.

Crystal data

C20H22BrFN2O	$\beta = 90.8535°$
$M_w = 405.31$	$V = 3878.03$ Å^3
Monoclinic, $P2_1/C$	$Z = 8$
$a = 10.7663$ Å	
$b = 33.0703$ Å	
$c = 10.8932$ Å	

Fractional atomic coordinates and isotropic displacement parameters (Å^2)

	x	y	z	U_{iso}
C1	0.627 03	0.907 95	0.621 28	0.057 70
C2	0.430 44	0.961 70	0.608 75	0.057 70
C3	0.560 60	0.912 80	0.511 33	0.057 70
C4	0.597 62	0.930 23	0.725 26	0.057 70
C5	0.498 98	0.957 52	0.719 01	0.057 70
C6	0.460 63	0.939 23	0.503 41	0.057 70
C7	0.328 29	0.989 41	0.602 40	0.058 40
N8	0.244 71	1.011 68	0.596 06	0.058 40
C9	0.616 59	0.885 90	0.415 44	0.058 40
O10	0.728 87	0.870 82	0.472 25	0.057 70
C11	0.724 56	0.875 10	0.604 48	0.057 70
C12	0.853 40	0.887 97	0.650 31	0.057 70
C13	0.910 63	0.870 68	0.753 89	0.058 40
C14	0.915 44	0.919 00	0.588 10	0.058 40
C15	1.031 95	0.932 47	0.628 13	0.057 70
C16	1.027 33	0.883 70	0.795 53	0.057 70
C17	0.677 62	0.835 40	0.662 19	0.057 70
C18	0.750 08	0.797 17	0.626 66	0.057 70
C19	0.739 97	0.765 49	0.727 96	0.057 70
N20	0.775 31	0.723 76	0.684 34	0.057 70
C21	0.670 93	0.703 61	0.615 98	0.057 70
C22	0.819 80	0.697 72	0.787 96	0.057 70
F23	1.199 91	0.927 25	0.772 13	0.058 40
C24	1.084 93	0.914 36	0.731 49	0.058 40

Continued

https://doi.org/10.1017/S0885715616000178 Published online by Cambridge University Press

TABLE II. Continued

Fractional atomic coordinates and isotropic displacement parameters (Å^2)

	x	y	z	U_{iso}
C25	0.048 44	0.585 01	0.690 59	0.058 40
C26	−0.149 07	0.545 04	0.580 08	0.058 40
C27	0.029 88	0.543 99	0.713 04	0.057 70
C28	−0.030 65	0.606 68	0.612 44	0.058 40
C29	−0.130 67	0.586 50	0.557 77	0.058 40
C30	−0.068 14	0.523 27	0.657 90	0.057 70
C31	−0.252 28	0.525 10	0.522 15	0.058 40
N32	−0.337 27	0.510 08	0.472 94	0.058 40
C33	0.127 72	0.529 27	0.801 91	0.057 70
O34	0.195 80	0.564 92	0.837 01	0.058 40
C35	0.160 13	0.599 92	0.764 69	0.058 40
C36	0.267 07	0.611 60	0.679 92	0.057 70
C37	0.455 34	0.629 54	0.518 31	0.058 40
C38	0.354 41	0.582 20	0.647 64	0.057 70
C39	0.276 10	0.650 22	0.627 70	0.058 40
C40	0.371 13	0.659 74	0.546 60	0.058 40
C41	0.449 36	0.590 78	0.566 00	0.058 40
C42	0.120 67	0.633 83	0.853 39	0.057 70
C43	0.221 27	0.646 32	0.946 91	0.058 40
C44	0.169 38	0.677 92	1.034 96	0.058 40
N45	0.267 00	0.696 64	1.118 05	0.058 40
C46	0.213 89	0.730 55	1.192 04	0.057 70
C47	0.331 52	0.666 95	1.200 19	0.057 70
F48	0.550 34	0.638 51	0.438 49	0.057 70
Br49	0.991 73	0.714 79	0.478 88	0.065 50
Br50	0.464 57	0.771 03	0.414 89	0.065 50
H51	0.649 99	0.926 86	0.810 31	0.074 30
H52	0.474 99	0.975 21	0.799 07	0.074 30
H53	0.405 27	0.942 60	0.420 06	0.075 00
H54	0.554 89	0.860 67	0.389 81	0.075 00
H55	0.867 44	0.846 45	0.804 75	0.075 00
H56	0.871 73	0.932 90	0.508 20	0.074 30
H57	1.081 67	0.956 21	0.581 06	0.074 30
H58	1.071 26	0.870 02	0.875 47	0.074 30
H59	0.581 38	0.831 18	0.631 72	0.075 00
H60	0.674 56	0.839 27	0.761 93	0.075 00
H61	0.848 08	0.803 80	0.610 58	0.074 30
H62	0.710 35	0.785 66	0.540 73	0.074 30
H63	0.645 68	0.762 88	0.763 13	0.074 30
H64	0.802 50	0.772 86	0.804 79	0.074 30
H65	0.705 72	0.675 64	0.576 42	0.074 30
H66	0.635 75	0.723 43	0.543 43	0.074 30
H67	0.596 92	0.697 54	0.680 83	0.074 30
H68	0.896 27	0.713 07	0.835 41	0.074 30
H69	0.850 13	0.668 83	0.750 86	0.072 00
H70	0.743 55	0.692 74	0.850 59	0.075 00
H71	0.848 78	0.726 07	0.622 57	0.075 00
H72	−0.015 44	0.638 49	0.592 10	0.075 00
H73	−0.194 18	0.602 54	0.496 85	0.043 00
H74	−0.084 58	0.491 48	0.674 85	0.075 00
H75	0.190 48	0.507 11	0.760 37	0.075 00
H76	0.088 79	0.515 44	0.884 17	0.074 30
H77	0.348 11	0.551 94	0.684 68	0.075 00
H78	0.208 65	0.673 52	0.647 98	0.075 00
H79	0.380 17	0.689 79	0.507 37	0.074 30
H80	0.515 12	0.567 67	0.539 45	0.075 00
H81	0.038 39	0.623 02	0.901 36	0.075 00
H82	0.091 04	0.660 13	0.799 24	0.074 30
H83	0.301 35	0.659 08	0.899 67	0.075 00
H84	0.252 03	0.619 36	0.996 83	0.074 30
H85	0.098 55	0.665 10	1.094 43	0.075 00
H86	0.127 96	0.703 28	0.984 56	0.075 00
H87	0.148 10	0.718 12	1.257 56	0.075 00
H88	0.165 92	0.751 30	1.129 51	0.074 30

Continued

https://doi.org/10.1017/S0885715616000178 Published online by Cambridge University Press

TABLE II. Continued

Fractional atomic coordinates and isotropic displacement parameters (Å^2)				
	x	*y*	*z*	U_{iso}
H89	0.289 75	0.745 50	1.241 96	0.075 00
H90	0.377 05	0.643 92	1.145 48	0.075 00
H91	0.263 31	0.652 94	1.259 58	0.075 00
H92	0.399 96	0.683 28	1.255 73	0.074 30
H93	0.333 82	0.709 02	1.059 43	0.075 00
H94	0.641 83	0.902 42	0.332 31	0.075 00

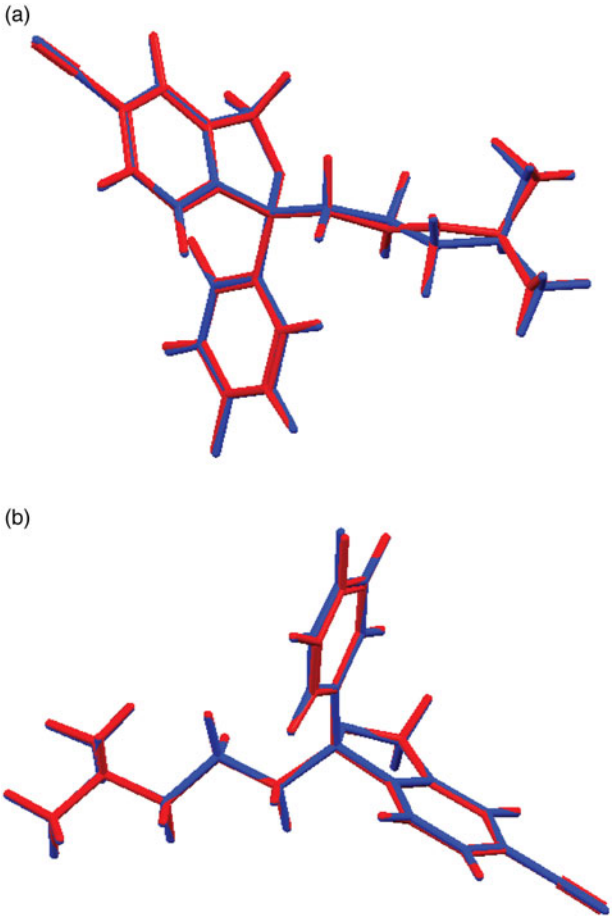

Figure 3. (Color online) Comparison of the refined and optimized structures of citalopram hydrobromide. The Rietveld refined structure is in red, and the DFT-optimized structure is in blue. (a) Cation 1. (b) Cation 2.

N-TREOR in EXPO2013 (Altomare *et al.*, 2013). Analysis of the systematic absences in EXPO2009 suggested the space group $P2_1/c$, which was confirmed by successful solution and refinement of the structure. A reduced cell search in the Cambridge Structural Database (Allen, 2002) combined with the chemistry "C H Br F N O only" yielded no hits. A name search on "citalopram" yielded (*S*)-citalopram oxalate oxalic acid hydrate (Harrison *et al.*, 2007, CSD Refcode SETVUJ; de Diego *et al.*, 2011, WASGAA) and (R*S*)-citalopram oxalate oxalic acid (de Diego *et al.*, 2011, WASGEE, and WASGEE01), and a connectivity search yielded the same four Refcodes.

A citalopram cation was built and its conformation optimized using Spartan '14 (Wavefunction, 2013), and saved as a mol2 file. This file was converted into a Fenske–Hall *Z*-matrix file using OpenBabel (O'Boyle *et al.*, 2011). Using the cation and a Br atom as fragments, the structure was solved with DASH (David *et al.*, 2006).

Rietveld refinement was carried out using GSAS (Toby, 2001; Larson and Von Dreele, 2004). Only the 1.0–25.0° portion of the pattern was included in the refinement (d_{min} = 0.955 Å).

All non-H bond distances and angles were subjected to restraints, based on a Mercury/Mogul Geometry Check (Bruno *et al.*, 2004; Sykes *et al.*, 2011) of the molecule. The Mogul average and standard deviation for each quantity were used as the restraint parameters. The rings C1–C6 (plus C7 and N8), C12–C16, C24 (plus F23), C25–C30 (plus C31 and N32), and C36–C41 (plus F48) were subjected to planar restraints. The restraints contributed 7.16% to the final χ^2. Isotropic displacement coefficients were refined, grouped by chemical similarity. The hydrogen atoms were included in calculated positions, which were recalculated during the

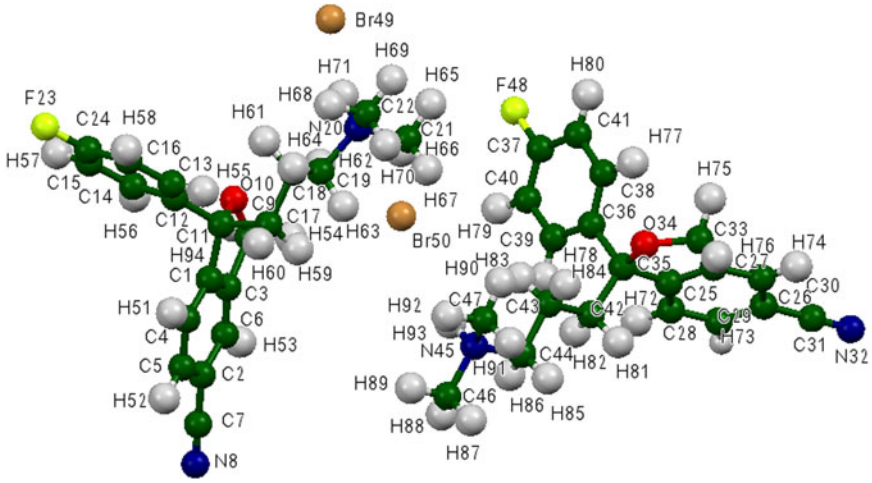

Figure 4. (Color online) The molecular structure of citalopram hydrobromide, with the atom numbering. The atoms are represented by 50% probability spheroids.

https://doi.org/10.1017/S0885715616000178 Published online by Cambridge University Press

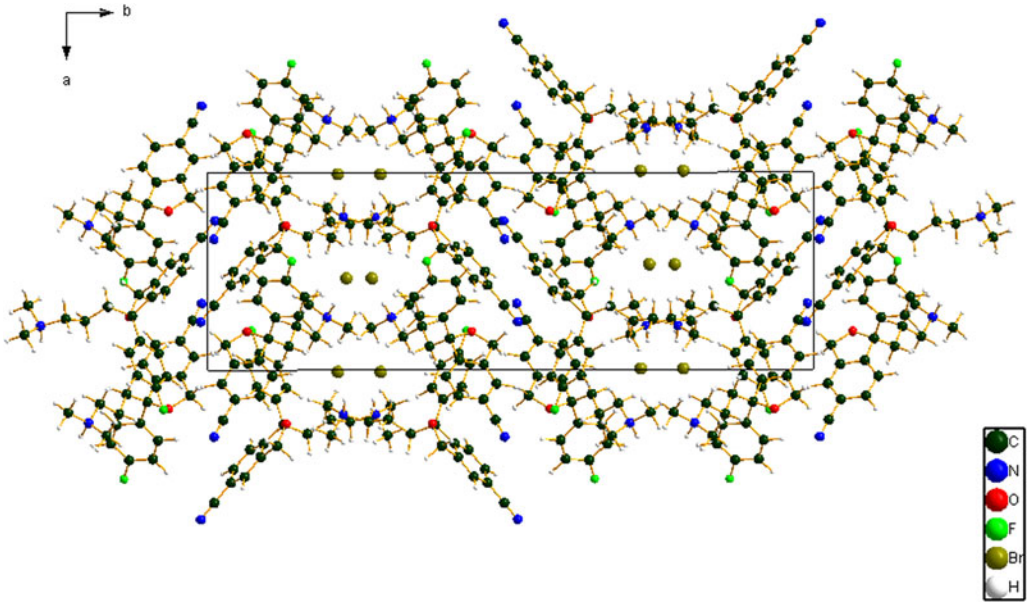

Figure 5. (Color online) The crystal structure of citalopram hydrobromide, viewed down the *c*-axis. The hydrogen bonds are shown as dashed lines.

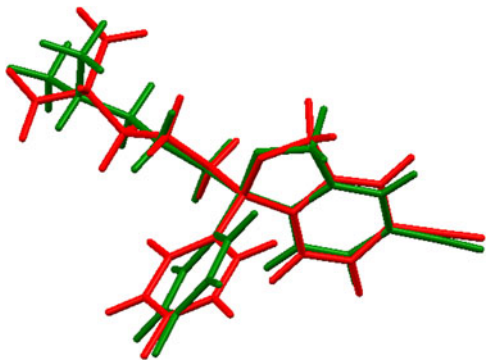

Figure 6. (Color online) Comparison of the two independent citalopram cations in the structure of citalopram hydrobromide. Cation 1 is in red and cation 2 is colored green.

refinement. The U_{iso} of each hydrogen atom was constrained to be 1.3× that of the heavy atom to which it is attached. The peak profiles were described using profile function #4 (Thompson *et al.*, 1987; Finger *et al.*, 1994), which includes the Stephens (1999) anisotropic strain broadening model. The background was modeled using a three-term shifted Chebyshev polynomial, with a five-term diffuse scattering function to model the Kapton capillary and any amorphous component. The refinement yielded the residuals $R_{wp} = 0.0792$, $R_p = 0.0649$, and $\chi^2 = 2.950$, but there were several unusual torsion angles in the side chain of one of the molecules. The final refinement of 184 variables [started from the results of the density functional theory (DFT) calculation] using 24 141 observations (24 003 data points and 138 restraints) yielded the residuals $R_{wp} = 0.0634$, $R_p = 0.0524$, and $\chi^2 = 1.860$. The largest peak (1.16 Å from F48) and hole (1.65 Å from C19) in the difference Fourier map were 0.34 and −0.35 $e(Å)^{-3}$, respectively. The Rietveld plot is included as Figure 2. The largest errors are in the positions and shapes of the low-angle peaks, and may indicate subtle changes in the sample during the measurement. The beamline staff indicated that the specimen darkened slightly during the measurement. A Le Bail fit yielded the residuals $R_{wp} = 0.0573$, $R_p = 0.0469$, and $\chi^2 = 1.520$. The Rietveld plot of the Le Bail fit is included as Supplementary Material. The largest errors in the fit were in the positions of certain strong low-angle peaks.

A density functional geometry optimization (fixed experimental unit cell) was carried out using CRYSTAL09 (Dovesi *et al.*, 2005). The basis sets for the H, C, N, and O atoms were those of Gatti *et al.* (1994), the basis set for F was that of Nada *et al.* (1993), and the basis set for Br was that of Peintinger *et al.* (2012). The calculation was run on eight 2.1 GHz Xeon cores (each with 6 GB RAM) of a 304-core Dell Linux cluster at IIT, used 8 *k*-points and the B3LYP functional, and took ∼5 days. The optimization changed the positions of one of the N–H hydrogen atoms significantly, resulting in a chemically more-reasonable structure.

III. RESULTS AND DISCUSSION

The powder pattern is similar enough to those reported by Ikemoto *et al.* (2001) to conclude that this citalopram hydrobromide is the same material crystallized by Sumika Fine Chemicals Co. Ltd in European Patent application

TABLE III. Hydrogen bonds in the DFT-optimized crystal structure of citalopram hydrobromide.

D–*H*···*A*	*D*–*H* (Å)	*H*···*A* (Å)	*D*···*A* (Å)	*D*–*H*···*A* (°)	Overlap (*e*)
N20–H71···Br49	1.049	2.243	3.268	165.4	0.054
N45–H93···Br50	1.052	2.228	3.272	171.7	0.060
C6–H53···O34	1.085	2.430	3.359	142.8	0.020

https://doi.org/10.1017/S0885715616000178 Published online by Cambridge University Press

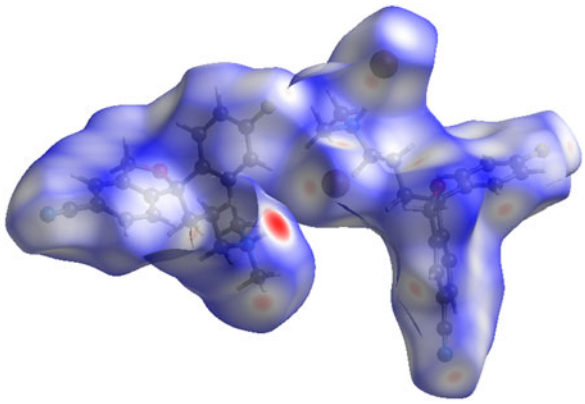

Figure 7. (Color online) The Hirshfeld surface of citalopram hydrobromide. Intermolecular contacts longer than the sums of the van der Waals radii are colored blue, and contacts shorter than the sums of the radii are colored red. Contacts equal to the sums of radii are white.

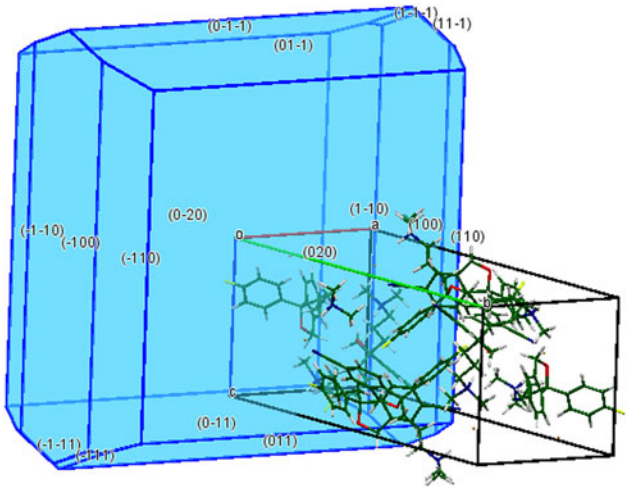

Figure 8. (Color online) The Bravais–Friedel–Donnay–Harker morphology of citalopram hydrobromide. The morphology is platy, with {010} as the major faces.

1,152,000. The refined atom coordinates (from the present study) of citalopram hydrobromide are reported in Table I, and the coordinates from the DFT optimization in Table II. The root-mean-square deviation of the non-hydrogen atoms in the citalopram cations are 0.126 and 0.057 Å respectively (Figure 3). The largest differences are in the cationic side chain of molecule 1. This excellent agreement between the refined and optimized structures is evidence that the experimental structure is correct (van de Streek and Neumann, 2014). This discussion uses the DFT-optimized structure. The asymmetric unit (with atom numbering) is illustrated in Figure 4, and the crystal structure is presented in Figure 5.

All of the bond distances, bond angles and torsion angles fall within the normal ranges indicated by a Mercury Mogul Geometry check (Macrae *et al.*, 2008). The root-mean-square displacement of the non-hydrogen atoms in the two independent cations is 0.500 Å (Figure 6). The largest differences are in the conformation of the cationic side chains and the fluorinated phenyl groups.

Quantum mechanical conformation examinations (Hartree–Fock/6-31G*/water) using Spartan '14 indicated that the observed conformations of the citalopram cations are within 3.0 kcal mole^{-1} in energy, and converge to the same minimum, which a molecular mechanics (MMFF) sampling of conformational space indicated was the minimum energy conformation.

Just as in this structure, there are two independent citalopram cations in the SETVUJ (Harrison *et al.*, 2007) and WASGAA (de Diego *et al.*, 2011) structures. The WASGEE and WASGEE01 structures (de Diego *et al.*, 2011) exhibit disorder, and will not be discussed further. The observed conformations in this structure are similar (but not identical) to the two conformations in SETVUJ and WASGAA.

Analysis of the contributions to the total crystal energy using the Forcite module of Materials Studio (Dassault, 2014) suggests that the intramolecular deformation energy is dominated by bond and angle distortion terms, as might be expected in a fused ring structure. The intermolecular energy contains significant contributions from both van der Waals and electrostatic contributions, which in this force-field-based analysis includes hydrogen bonds. The hydrogen bonds are better analyzed using the results of the DFT calculation (Table III).

As expected, both N–H cationic groups form discrete hydrogen bonds to the bromide cations, with graph sets *D1,1*(2) (Etter, 1990; Bernstein *et al.*, 1995; Shields *et al.*, 2000). A C–H···O hydrogen bond between a phenyl carbon and the ring oxygen O34 apparently also contributes significantly to the crystal energy.

The volume enclosed by the Hirshfeld surface (Figure 7; Hirshfeld, 1977; McKinnon *et al.*, 2004; Spackman and Jayatilaka, 2009; Wolff *et al.*, 2012) is 955.26 Å^3, 98.53% of 1/4 the unit-cell volume. The molecules are thus not tightly packed. The only significant close contacts (red in Figure 7) involve the hydrogen bonds.

The Bravais–Friedel–Donnay–Harker (Bravais, 1866; Friedel, 1907; Donnay and Harker, 1937) morphology suggests that we might expect platy morphology for citalopram hydrobromide, with {010} as the principal faces (Figure 8). A forth-order spherical harmonic preferred orientation model was included in the refinement; the texture index was only 1.002, indicating that preferred orientation was not significant in this rotated capillary specimen. The powder pattern of citalopram hydrobromide has been published in the ICDD Powder Diffraction File, entry 00-065-1422.

SUPPLEMENTARY MATERIAL

The supplementary material for this article can be found at http://dx.doi.org/10.1017/S0885715616000178.

ACKNOWLEDGEMENTS

Use of the Advanced Photon Source at Argonne National Laboratory was supported by the U. S. Department of Energy, Office of Science, Office of Basic Energy Sciences, under Contract No. DE-AC02-06CH11357. This work was partially supported by the International Centre for Diffraction Data. We thank Lynn Ribaud for his assistance in data collection, and Andrey Rogachev for the use of computing resources at IIT.

Allen, F. H. (**2002**). "The Cambridge Structural Database: a quarter of a million crystal structures and rising," Acta Crystallogr. Sect. B: Struct. Sci. **58**, 380–388.

Altomare, A., Cuocci, C., Giacovazzo, C., Moliterni, A., Rizzi, R., Corriero, N., and Falcicchio, A. (**2013**). "EXPO2013: a kit of tools for phasing crystal structures from powder data", J. Appl. Crystallogr. **46**, 1231–1235.

Bernstein, J., Davis, R. E., Shimoni, L., and Chang, N. L. (**1995**). "Patterns in hydrogen bonding: functionality and graph set analysis in crystals," Angew. Chem. Int. Ed. Engl. **34**(15), 1555–1573.

Bogeso, K. P. and Lundbeck, H. (**1987**). "Novel Intermediate and Method for Its Preparation," US Patent 4,650,884.

Bravais, A. (**1866**). *Etudes Cristallographiques* (Gauthier Villars, Paris).

Bruno, I. J., Cole, J. C., Kessler, M., Luo, J., Motherwell, W. D. S., Purkis, L. H., Smith, B. R., Taylor, R., Cooper, R. I., Harris, S. E., and Orpen, A. G. (**2004**). "Retrieval of crystallographically-derived molecular geometry information," J. Chem. Inf. Sci. **44**, 2133–2144.

Dassault Systèmes (**2014**). *Materials Studio 8.0* (BIOVIA, San Diego, CA).

David, W. I. F., Shankland, K., van de Streek, J., Pidcock, E., Motherwell, W. D. S., and Cole, J. C. (**2006**). "DASH: a program for crystal structure determination from powder diffraction data," J. Appl. Crystallogr. **39**, 910–915.

de Diego, H. L., Bond, A. D., and Dancer, R. J. (**2011**). "Formation of solid solutions between racemic and enantiomeric citalopram oxalate," Chirality **23**(5), 408–416.

Donnay, J. D. H. and Harker, D. (**1937**). "A new law of crystal morphology extending the law of Bravais," Amer. Mineral. **22**, 446–467.

Dovesi, R., Orlando, R., Civalleri, B., Roetti, C., Saunders, V. R., and Zicovich-Wilson, C. M. (**2005**). "CRYSTAL: a computational tool for the *ab initio* study of the electronic properties of crystals," Z. Kristallogr. **220**, 571–573.

Etter, M. C. (**1990**). "Encoding and decoding hydrogen-bond patterns of organic compounds," Acc. Chem. Res. **23**(4), 120–126.

Finger, L. W., Cox, D. E., and Jephcoat, A. P. (**1994**). "A correction for powder diffraction peak asymmetry due to axial divergence," J. Appl. Crystallogr. **27**(6), 892–900.

Friedel, G. (**1907**). "Etudes sur la loi de Bravais," Bull. Soc. Fr. Mineral. **30**, 326–455.

Gatti, C., Saunders, V. R., and Roetti, C. (**1994**). "Crystal-field effects on the topological properties of the electron-density in molecular crystals – the case of urea," J. Chem. Phys. **101**, 10686–10696.

Harrison, W. T., Yathirajan, H. S., Bindya, S., and Anilkumar, H. G. (**2007**). "Escitalopram oxalate: co-existence of oxalate dianions and oxalic acid molecules in the same crystal," Acta Crystallogr. Sect. C: Crystal Struct. Commun. **63**(2), o129–o131.

Hirshfeld, F. L. (**1977**). "Bonded-atom fragments for describing molecular charge densities," Theor. Chem. Acta **44**, 129–138.

ICDD (**2015**), PDF-4+ 2014 (Database), edited by Dr. Soorya Kabekkodu, International Centre for Diffraction Data, Newtown Square, PA, USA.

Ikemoto, T., Arai, N., and Igi, M. (**2001**). "Citalopram hydrobromide crystal and method for crystallization thereof," European Patent Application EP 1,152,000.

Larson, A. C. and Von Dreele, R. B. (**2004**). *General Structure Analysis System, (GSAS)*, (Los Alamos National Laboratory Report LAUR 86-784).

Lee, P. L., Shu, D., Ramanathan, M., Preissner, C., Wang, J., Beno, M. A., Von Dreele, R. B., Ribaud, L., Kurtz, C., Antao, S. M., Jiao, X., and Toby, B. H. (**2008**). "A twelve-analyzer detector system for high-resolution powder diffraction," J. Synchroton Radiat. **15**(5), 427–432.

Macrae, C. F., Bruno, I. J., Chisholm, J. A., Edington, P. R., McCabe, P., Pidcock, E., Rodriguez-Monge, L., Taylor, R., van de Streek, J., and Wood, P. A. (**2008**). "Mercury CSD 2.0 – new features for the visualization and investigation of crystal structures," J. Appl. Crystallogr. **41**, 466–470.

McKinnon, J. J., Spackman, M. A., and Mitchell, A. S. (**2004**). "Novel tools for visualizing and exploring intermolecular interactions in molecular crystals," Acta Crystallogr. Sect. B: Struct. Sci. **60**, 627–668.

Nada, R., Catlow, C. R. A., Pisani, C., and Orlando, R. (**1993**). "Ab initio Hartree-Fock perturbed-cluster study of neutral defects in LiF," Model. Simul. Mater. Sci. Eng. **1**, 165–187.

O'Boyle, N., Banck, M., James, C. A., Morley, C., Vandermeersch, and Hutchison, G. R. (**2011**). "Open babel: an open chemical toolbox," J. Chem. Inf., **3**, 33. doi: 10.1186/1758-2946-3-33.

Peintinger, M. F., Vilela Oliveira, D., and Bredow, T. (**2012**). "Consistent gaussian basis sets of triple-zeta valence with polarization quality for solid-state calculations," J. Comput. Chem. **34**(6), 451–459. doi: 10.1002/jcc.23153

Shields, G. P., Raithby, P. R., Allen, F. H., and Motherwell, W. S. (**2000**). "The assignment and validation of metal oxidation states in the Cambridge Structural Database," Acta Crystallogr. Sect. B: Struct. Sci. **56**(3), 455–465.

Spackman, M. A. and Jayatilaka, D. (**2009**). "Hirshfeld surface analysis," CrystEngComm **11**, 19–32.

Stephens, P. W. (**1999**). "Phenomenological model of anisotropic peak broadening in powder diffraction," J. Appl. Crystallogr. **32**, 281–289.

Sykes, R. A., McCabe, P., Allen, F. H., Battle, G. M., Bruno, I. J., and Wood, P. A. (**2011**). "New software for statistical analysis of Cambridge Structural Database data," J. Appl. Crystallogr. **44**, 882–886.

Thompson, P., Cox, D. E., and Hastings, J. B. (**1987**). "Rietveld refinement of Debye–Scherrer synchrotron X-ray data from Al_2O_3," J. Appl. Crystallogr. **20**(2), 79–83.

Toby, B. H. (**2001**). "EXPGUI, a graphical user interface for GSAS," J. Appl. Crystallogr. **34**, 210–213.

van de Streek, J. and Neumann, M. A. (**2014**). "Validation of molecular crystal structures from powder diffraction data with dispersion-corrected density functional theory (DFT-D)," Acta Crystallogr. Sect. B: Struct. Sci. **70**(6), 1020–1032.

Wang, J., Toby, B. H., Lee, P. L., Ribaud, L., Antao, S. M., Kurtz, C., Ramanathan, M., Von Dreele, R. B., and Beno, M. A. (**2008**). "A dedicated powder diffraction beamline at the Advanced Photon Source: commissioning and early operational results," Rev. Sci. Instrum. **79**, 085105.

Wavefunction, Inc. (**2013**). Spartan '14 Version 1.1.0, Wavefunction Inc., 18401 Von Karman Ave., Suite 370, Irvine CA 92612.

Wolff, S. K., Grimwood, D. J., McKinnon, M. J., Turner, M. J., Jayatilaka, D., and Spackman, M. A. (**2012**). CrystalExplorer *Version 3.1* (University of Western Australia).